PHYSICAL REVIEW B VOLUME 50, NUMBER 11 15 SEPTEMBER 1994-I

Direct derivation of effective-mass equations for microstructures with atomically abrupt boundaries

M. G. Burt
BT Laboratories, Martlesham Heath, Ipswich, Suffolk IP5 7RE, United Kingdom
(Received 23 March 1994)

A direct general method for deriving effective-mass equations for microstructures with atomically abrupt boundaries is presented. The principal assumption is that the envelope functions are slowly varying on the scale of the lattice period. The band-edge Bloch functions are not assumed to be the same on both sides of an interface and it is shown how the differences can be taken into account perturbatively. The particle in a box method is known to work well in many situations. To demonstrate why, a derivation of the effective-mass equation is carried out explicitly for the case of conduction-band states of a type-I microstructure composed of zinc-blende crystals without spin-orbit interaction. The derivation provides much insight into why the effective-mass method works so well. The method is illustrated by applying it to a one-dimensional superlattice problem. For this model problem, the effective-mass approximation to the wave function is seen to be good even for a quantum well one lattice period wide.

I. INTRODUCTION

The particle in a box model, with various degrees of refinement (see, e.g., Refs. 1–4, and references therein), is in extensive use for calculating the energy levels and envelope functions of electronic states in semiconductor microstructures and the justification for its use is an important issue. In trying to justify the model, it is usual (see, e.g., Refs. 1–3) to assume that the corresponding band-edge Bloch functions in the materials comprising the microstructure are sufficiently similar for the differences between them to be neglected. However, it has recently pointed out[5] that for cases of practical interest this is not a reasonable assumption because it requires the neglect of terms of the same order of magnitude or even larger than those retained in conventional derivations. Furthermore, it has been shown how to rectify the situation by developing an exact envelope function method[5–7] for microstructures and using it to derive an effective-mass equation without neglecting the above-mentioned differences in the band-edge Bloch functions.[5] This exact envelope-function method has been applied recently[8] to the problems of calculating quantum-well valence-band states to overcome difficulties arising from the use of heuristic methods. What is clearly desirable is to find a more direct method for deriving effective-mass equations, one that avoids the need to formulate an exact envelope-function method in the first place, and yet still incorporates the differences between corresponding Bloch functions of the materials of which the microstructure is composed. It is the purpose of this paper to show how this can be done using an example that adds insight into why the particle in a box model works so well.

Section II shows how approximate envelope-function equations can be derived for microstructures using only the slowly varying nature of the envelope functions. In Sec. III, the derivation of the effective-mass equation is carried out explicitly for the case of conduction-band states of a type-I microstructure composed of zinc-blende crystals ignoring the spin-orbit interaction. In Sec. IV, the method is illustrated using a one-dimensional superlattice model composed of "Mathieu" crystals, i.e., those for which the microscopic potential, apart from a constant, is a cosine. It will be shown that the effective-mass method works for this model system even for structures with wells only one lattice period wide. The discussion in Sec. V adds insight into why the effective-mass method works so well.

II. DERIVATION OF THE APPROXIMATE ENVELOPE-FUNCTION EQUATIONS

The problem we consider is as follows. Take a Bravais lattice with primitive lattice vectors $\mathbf{a}_1$, $\mathbf{a}_2$, and $\mathbf{a}_3$ and denote the position vector $\mathbf{r}$ by $\mathbf{r}=r_1\mathbf{a}_1+r_2\mathbf{a}_2+r_3\mathbf{a}_3$. Define the $\mathbf{n}$th unit cell, $\mathbf{n}=(n_1,n_2,n_3)$ where the n_i are integers, as the volume defined by $n_i \le r_i < n_i+1$, $i=1,2,3$. Our idealized microstructure is then defined by specifying the element or compound occupying the $\mathbf{n}$th unit cell. For instance, for a microstructure in the $GaAs/Ga_xAl_{1-x}As$ material system one would specify the value of x (including the possibility $x=0$) for each unit cell, i.e., one could regard x as a function $x(\mathbf{n})$ of the integer variable $\mathbf{n}$. The potential inside the $\mathbf{n}$th unit cell is just the bulk potential corresponding to the element or compound occupying that cell with perhaps an additive constant to take account of band offsets. The potential is, therefore, piecewise periodic with the discontinuities appearing at the boundaries of unit cells corresponding to a change of composition. Returning to the example of the $GaAs/Ga_xAl_{1-x}As$ material system, the potential inside the $\mathbf{n}$th unit cell of the microstructure is

$$V_0(\mathbf{n})+\sum_{\mathbf{G}}\tilde{V}_{\mathbf{G}}[x(\mathbf{n})]e^{i\mathbf{G}\cdot\mathbf{r}}\ , \tag{1}$$

where $\sum_{\mathbf{G}}\tilde{V}_{\mathbf{G}}(x)e^{i\mathbf{G}\cdot\mathbf{r}}$ ($\mathbf{G}$ being a reciprocal lattice vector) is the potential for bulk $Ga_xAl_{1-x}As$ and $V_0(\mathbf{n})$ is constant for each unit cell to take account of band offsets.

We start with the Schrödinger equation in the plane-

wave representation. The wave function is expanded in plane waves

$$\psi(\mathbf{r})=\sum_{\mathbf{kG}}\tilde{\psi}_{\mathbf{G}}(\mathbf{k})e^{i(\mathbf{k}+\mathbf{G})\cdot\mathbf{r}}\ , \tag{2}$$

where the wave vector has been expressed as $\mathbf{k}+\mathbf{G}$, $\mathbf{G}$ being a reciprocal lattice vector of the underlying Bravais lattice and $\mathbf{k}$ is inside a Brillouin zone defined with respect to that lattice. (Cyclic boundary conditions are applied to a large macroscopic volume completely enclosing the microstructure.) The Schrödinger equation in this representation is

$$\frac{\hbar^2}{2m}(\mathbf{k}+\mathbf{G})^2\tilde{\psi}_{\mathbf{G}}(\mathbf{k})+\sum_{\mathbf{k'G'}}\langle\mathbf{k}+\mathbf{G}|V|\mathbf{k'}+\mathbf{G'}\rangle\tilde{\psi}_{\mathbf{G'}}(\mathbf{k'})=E\tilde{\psi}_{\mathbf{G}}(\mathbf{k})\ , \tag{3}$$

where V is the microscopic potential. Now we are interested in slowly varying solutions, i.e., those for which $\tilde{\psi}_{\mathbf{G}}(\mathbf{k})$ is only appreciable for small $\mathbf{k}$. For small $\mathbf{k}$ and $\mathbf{k'}$ (and indeed for any $\mathbf{k}$ and $\mathbf{k'}$ for which $\mathbf{k}-\mathbf{k'}$ is within the Brillouin zone) one can write

$$\langle\mathbf{k}+\mathbf{G}|V|\mathbf{k'}+\mathbf{G'}\rangle=\tilde{V}_{\mathbf{G}-\mathbf{G'}}(\mathbf{k}-\mathbf{k'})\ , \tag{4}$$

where the $\tilde{V}_{\mathbf{G}}(\mathbf{k})$ are the plane-wave expansion coefficients of $V(\mathbf{r})$, i.e.,

$$V(\mathbf{r})=\sum_{\mathbf{kG}}\tilde{V}_{\mathbf{G}}(\mathbf{k})e^{i(\mathbf{k}+\mathbf{G})\cdot\mathbf{r}}\ . \tag{5}$$

So our slowly varying solutions of (3) will certainly obey

$$\frac{\hbar^2}{2m}(\mathbf{k}+\mathbf{G})^2\tilde{\psi}_{\mathbf{G}}(\mathbf{k})+\sum_{\mathbf{k'G'}}\tilde{V}_{\mathbf{G}-\mathbf{G'}}(\mathbf{k}-\mathbf{k'})\tilde{\psi}_{\mathbf{G'}}(\mathbf{k'})=E\tilde{\psi}_{\mathbf{G}}(\mathbf{k}) \tag{6}$$

to a high accuracy. If we now transform into real space, i.e., change to the new dependent variables

$$\psi_{\mathbf{G}}(\mathbf{r})=\sum_{\mathbf{k}}\tilde{\psi}_{\mathbf{G}}(\mathbf{k})e^{i\mathbf{k}\cdot\mathbf{r}}\ , \tag{7}$$

we get

$$-\frac{\hbar^2}{2m}\nabla^2\psi_{\mathbf{G}}(\mathbf{r})-i\frac{\hbar^2}{m}\mathbf{G}\cdot\nabla\psi_{\mathbf{G}}(\mathbf{r})+\frac{\hbar^2\mathbf{G}^2}{2m}\psi_{\mathbf{G}}(\mathbf{r})+\sum_{\mathbf{G}}\mathbf{V}_{\mathbf{G}-\mathbf{G'}}(\mathbf{r})\psi_{\mathbf{G'}}(\mathbf{r})=E\psi_{\mathbf{G}}(\mathbf{r}). \tag{8}$$

Of course, in transforming into real space, the sum over $\mathbf{k}$ in (7) and that over $\mathbf{k'}$ in (6) must be extended to all wave vectors, not just those inside the Brillouin zone, but this introduces little error because we are only interested in slowly varying solutions $\psi_{\mathbf{G}}(\mathbf{r})$ of (8) so that $\tilde{\psi}_{\mathbf{G}}(\mathbf{k})$ is only appreciable for small $\mathbf{k}$. As we will now show, if $\tilde{V}_{\mathbf{G}-\mathbf{G'}}(\mathbf{k}-\mathbf{k'})$ is approximated by a certain expression valid for small $\mathbf{k}-\mathbf{k'}$, then $V_{\mathbf{G}-\mathbf{G'}}(\mathbf{r})$ is just the plane-wave expansion coefficient (for wave vector $\mathbf{G}-\mathbf{G'}$) for the bulk crystal potential (including the constant part to take account of band offsets) of the element and/or compound occupying the unit cell contain $\mathbf{r}$. $V_{\mathbf{G}-\mathbf{G'}}(\mathbf{r})$ changes abruptly across the boundary between two unit cells if the material composition does the same, i.e., it is piecewise constant because the microscopic potential is piecewise periodic.

To show how the plane-wave expansion coefficients $\tilde{V}_{\mathbf{G}-\mathbf{G'}}(\mathbf{k}-\mathbf{k'})$ are approximated, we use a one-dimensional example in the first instance. We start with a plane-wave expansion for the microscopic potential V

$$V(x)=\sum_{kG}\tilde{V}_G(k)e^{i(k+G)x}\ , \tag{9a}$$

$$\tilde{V}_G(k)=\frac{1}{L}\int V(x)e^{-i(k+G)x}dx\ , \tag{9b}$$

where L is the large length over which cyclic boundary conditions are imposed. Suppose the region $x=na$ to $x=n'a$, where a is the lattice period, is occupied by a "crystal" of one type, i.e., the potential is periodic in that region and given by $\sum_{G''}V_{G''}^{(\text{crystal})}e^{iG''x}$. (The constant potential to take account of the band offsets can be contained in the $G''=0$ term.) The contribution to $\tilde{V}_G(k)$ would be given by

$$i\sum_{G''}V_{G''}^{(\text{crystal})}\frac{e^{-ikn'a}-e^{-ikna}}{(k+G-G'')L}\ , \tag{10}$$

where we have used the fact that G and G'' are reciprocal lattice vectors so that $e^{iGna}=1$. Now, to evaluate $\tilde{V}_G(k)$ for small k, we need to retain only the term corresponding to $G''=G$, i.e.,

$$iV_G^{(\text{crystal})}\frac{e^{-ikn'a}-e^{-ikna}}{kL} \tag{11}$$

is a good approximation to (10). But this is just the plane-wave expansion coefficient for a function that is constant and equal to $V_G^{(\text{crystal})}$ for x between na and $n'a$ and zero elsewhere. Clearly each crystal layer will contribute a similar term; in each layer the $V_G(x)$ will just be the value of $V_G^{(\text{crystal})}$ appropriate for the crystal occupying the layer. So, if in the region between $x=na$ and $x=n'a$, the microscopic potential is $\sum_{G''}V_{G''}^{(A)}e^{iG''x}$ corresponding to material A, and elsewhere the microscopic potential is $\sum_{G''}V_{G''}^{(B)}e^{iG''x}$ corresponding to material B, then in the region between $x=na$ and $x=n'a$ $V_G(x)$ will be equal to $V_G^{(A)}$, but equal to $V_G^{(B)}$ everywhere else.

The extension to three dimensions is straightforward. The position vector $\mathbf{r}$ is expressed as $r_1\mathbf{a}_1+r_2\mathbf{a}_2+r_3\mathbf{a}_3$, where the $\mathbf{a}_i$ are the primitive lattice vectors of the underlying Bravis lattice. We suppose that in the unit cells within the parallelepiped defined by $n_j<r_j\le n_j'$, $j=1,2,3$, the microscopic potential is given by $\sum_{\mathbf{G}''}V_{\mathbf{G}''}^{(A)}e^{i\mathbf{G}''\cdot\mathbf{r}}$, i.e., the region is occupied by material A. The contribution to $\tilde{V}_{\mathbf{G}}(\mathbf{k})$ from this region is

$$i^3J\sum_{\mathbf{G}''}V_{\mathbf{G}''}^{(A)}\prod_{j=1}^{j=3}\frac{e^{-ik_jn_j'}-e^{-ik_jn_j}}{(k_j+G_j-G_j'')L_j}\ , \tag{12}$$

where the wave vector $\mathbf{k}+\mathbf{G}$ is written as $\sum_{j=1}^{3}(k_j+G_j)\mathbf{b}_j$ and the $\mathbf{b}_j$ are the reciprocal lattice vectors. We have made use of the fact that the G_j's are integers to simplify the arguments of the exponentials. Cy-

clic boundary conditions are taken over a large parallelepiped of which the jth side is composed of L_j unit cells. J is the Jacobian for the coordinate system, i.e., the volume element is $J\,dr_1dr_2dr_3$. For small $\mathbf{k}$ the dominant term in (12) is the one with $\mathbf{G}''=\mathbf{G}$, i.e.,

$$i^3 J V_{\mathbf{G}}^{(A)} \prod_{j=1}^{j=3} \frac{e^{-ik_j n_j'} - e^{-ik_j n_j}}{k_j L_j} , \tag{13}$$

and it will be a good approximation thereto. The quantity (13) is equal to the fourier transform of the function that is equal to $V_{\mathbf{G}}^{(A)}$ in the region defined by $n_j < r_j \leq n_j'$, $j=1,2,3$ and zero elsewhere. It is clear, therefore, that for a general structure $V_{\mathbf{G}-\mathbf{G}'}(\mathbf{r})$ will equal the bulk value for the material occupying the unit cell in which $\mathbf{r}$ is located when we use the small wave-vector approximation (13) for (12). This will hold even if a microstructure is composed of bulk material in which just one unit cell is replaced by that of another material.

To proceed with the derivation of the approximate envelope function and effective-mass equations, it is now convenient to change to the envelope-function variables

$$F_n(\mathbf{r}) = \sum_{\mathbf{G}} U_{n\mathbf{G}}^* \psi_{\mathbf{G}}(\mathbf{r}) , \tag{14}$$

where the $U_{n\mathbf{G}}$ are orthonormal and complete

$$\sum_{\mathbf{G}} U_{n\mathbf{G}}^* U_{n'\mathbf{G}} = \delta_{n,n'} , \tag{15a}$$

$$\sum_{n} U_{n\mathbf{G}}^* U_{n\mathbf{G}'} = \delta_{\mathbf{G},\mathbf{G}'} . \tag{15b}$$

From (2) and (7), the approximate wave function is given by

$$\psi(\mathbf{r}) = \sum_{\mathbf{G}} \psi_{\mathbf{G}}(\mathbf{r}) e^{i\mathbf{G}\mathbf{r}} = \sum_{n} F_n(\mathbf{r}) U_n(\mathbf{r}) , \tag{16}$$

where the periodic basis functions $U_n(\mathbf{r})$ are given by

$$U_n(\mathbf{r}) = \sum_{\mathbf{G}} U_{n\mathbf{G}} e^{i\mathbf{G}\mathbf{r}} . \tag{17}$$

One choice for the $U_n(\mathbf{r})$ could be the zone-center eigenfunctions of one of the constituent materials. Premultiplying (8) by $U_{n\mathbf{G}}^*$ and summing over all $\mathbf{G}$, and using (14) and (15b) (completeness) gives

$$-\frac{\hbar^2}{2m}\nabla^2 F_n(\mathbf{r}) - i\frac{\hbar}{m}\sum_{n'} \mathbf{p}_{nn'}\cdot\nabla F_{n'}(\mathbf{r}) + \sum_{n'} H_{nn'}(\mathbf{r}) F_{n'}(\mathbf{r}) = E F_n(\mathbf{r}) , \tag{18}$$

where the $\mathbf{p}_{nn'}$ are matrix elements of momentum with respect to the periodic functions $U_n(\mathbf{r})$

$$\mathbf{p}_{nn'} = \sum_{\mathbf{G}} U_{n\mathbf{G}}^* \hbar\mathbf{G} U_{n'\mathbf{G}} \tag{19}$$

and the $H_{nn'}(\mathbf{r})$ are the corresponding matrix elements of the periodic crystal Hamiltonian of the material at $\mathbf{r}$

$$H_{nn'}(\mathbf{r}) = \sum_{\mathbf{G}\mathbf{G}'} U_{n\mathbf{G}}^* \left[\frac{\hbar^2\mathbf{G}^2}{2m}\delta_{\mathbf{G}\mathbf{G}'} + V_{\mathbf{G}-\mathbf{G}'}(\mathbf{r}) \right] U_{n'\mathbf{G}'} . \tag{20}$$

Clearly $H_{nn'}(\mathbf{r})$ will have the same piecewise constant form as the $V_{\mathbf{G}-\mathbf{G}'}(\mathbf{r})$. $H_{nn'}(\mathbf{r})$ will equal the value for the bulk material occupying the unit cell in which $\mathbf{r}$ is located. The diagonal elements will contain the constant term that takes the band offsets into account.

III. DERIVATION OF THE EFFECTIVE-MASS EQUATION

Now, provided the materials of which the microstructure is composed are not too disparate, then one can choose the $U_n(\mathbf{r})$ so that the off-diagonal elements of $H_{nn'}(\mathbf{r})$ are small [e.g., $U_n(\mathbf{r})$ could be the nth zone-center Bloch function for the well material in a quantum-well problem]. In such cases, it is possible to derive effective-mass equations from the approximate envelope-function equations in the usual way[9] by eliminating small envelope functions in favor of the dominant one(s), but being careful[5] to include the off-diagonal elements $H_{nn'}(\mathbf{r})$. At first sight it would appear that the presence of the off-diagonal elements in $H_{nn'}(\mathbf{r})$ would prevent one from deriving the effective-mass equation because of the appearance of products of $H_{nn''}(\mathbf{r})$ and $\mathbf{p}_{n''n'}$. It has been mentioned elsewhere,[5] in general terms, how a combination of time reversal and space symmetries reduce the importance of such terms. It is instructive to consider a simple example that illustrates this point *a fortiori*. Take a microstructure composed of direct-gap zinc-blende semiconductors without spin-orbit interaction and derive the effective-mass equation for the conduction-band states. To derive the effective-mass equation we start with (18) with $n=c$, the conduction band

$$-\frac{\hbar^2}{2m}\nabla^2 F_c(\mathbf{r}) - i\frac{\hbar}{m}\sum_{r(\Gamma_{15})} \mathbf{p}_{cr}\cdot\nabla F_r(\mathbf{r}) + H_{cc}(\mathbf{r})F_c(\mathbf{r}) + \sum_{r(\Gamma_1)} H_{cr}(\mathbf{r})F_r(\mathbf{r}) = E F_c(\mathbf{r}) , \tag{21}$$

where the sum over r denotes a sum over "remote" bands, i.e., all bands other than the conduction band. We have left out the term involving $\mathbf{p}_{cc}$ because the latter is zero by symmetry. The sum in the second (momentum) term on the left-hand side (lhs) of (21) is restricted to terms corresponding to basis functions U_r of Γ_{15} symmetry because all the other terms are zero. Similarly the sum in the last term on the lhs is restricted to basis functions of Γ_1 symmetry. The small envelope functions F_r are found from (18) with $n=r$

$$F_r(\mathbf{r}) \approx [E - H_{rr}(\mathbf{r})]^{-1} \left[-\frac{i\hbar}{m}\mathbf{p}_{rc}\cdot\nabla F_c(\mathbf{r}) + H_{rc}(\mathbf{r})F_c(\mathbf{r}) \right] . \tag{22}$$

We only get a nonzero F_r for r corresponding to a basis function of either Γ_1 or Γ_{15} symmetry. For Γ_1 symmetry one gets

$$F_r(\mathbf{r}) \approx [E - H_{rr}(\mathbf{r})]^{-1} H_{rc}(\mathbf{r}) F_c(\mathbf{r}) \tag{23a}$$

and for Γ_{15} symmetry

$$F_r(\mathbf{r}) \approx [E - H_{rr}(\mathbf{r})]^{-1} \left[-\frac{i\hbar}{m} \mathbf{p}_{rc} \cdot \nabla F_c(\mathbf{r}) \right] . \quad (23b)$$

Using (23a) and (23b) in (21) gives

$$-\frac{\hbar^2}{2m} \nabla \cdot \left[\frac{1}{m_c(E,\mathbf{r})} \nabla F_c(\mathbf{r}) \right] + H_{cc}^{(2)}(E,\mathbf{r}) F_c(\mathbf{r}) = E F_c(\mathbf{r}) , \quad (24)$$

where the energy-dependent effective mass $m_c(E,\mathbf{r})$ is given by

$$\frac{m}{m_c(E,\mathbf{r})} = 1 + \frac{2}{m} \sum_{r(\Gamma_{15})} p_{cr} [E - H_{rr}(\mathbf{r})]^{-1} p_{rc} , \quad (25)$$

with p standing for the component of the momentum along one of the cubic axes. $H_{cc}^{(2)}(E,\mathbf{r})$ is the conduction-band edge at $\mathbf{r}$ calculated to second order, i.e.,

$$H_{cc}^{(2)}(E,\mathbf{r}) = H_{cc}(\mathbf{r}) + \sum_{r(\Gamma_1)} H_{cr}(\mathbf{r}) [E - H_{rr}(\mathbf{r})]^{-1} H_{rc}(\mathbf{r}) . \quad (26)$$

So we see that the symmetry in this case has allowed us to take into account, via the off-diagonal elements of $H_{nn'}(\mathbf{r})$, the fact that the zone-center Bloch functions of the constituent materials are not the same and yet still retain the effective-mass form (24). Note that both $m_c(E,\mathbf{r})$ and $H_{cc}^{(2)}(E,\mathbf{r})$ are piecewise constant because the $H_{nn'}(\mathbf{r})$ are piecewise constant for the piecewise-periodic microscopic potential assumed.

At first sight it would appear that in establishing Eq. (24) with the defining Eqs. (25) and (26) much of the simplicity of the effective-mass approach has been lost. In particular, it would seem that one now needs a plethora of new parameters to calculate the quantities $m_c(E,\mathbf{r})$ and $H_{cc}^{(2)}(E,\mathbf{r})$. In practice, however, this is not likely to be necessary as these quantities are well approximated by the experimental effective mass and the conduction-band edge. It is interesting to note that the position dependence of the effective mass defined by $m_c(E,\mathbf{r})$ is determined entirely by the energy denominator in (25); the momentum matrix elements are the same throughout the structure. To include the effect of the dependence of the interband matrix elements on material one has to carry out the above perturbation analysis to the next order so as to include terms of third order in small quantities. However, when this is done the effective-mass form (24) is lost.

IV. NUMERICAL EXAMPLES

To illustrate the algebraic work in the previous section, the differences between the effective-mass approximation to the wave function and the exact wave function will be computed for a model one-dimensional type-I superlattice. The component crystals of this superlattice have a microscopic potential of the "Mathieu" form $V_0 + V_S \cos(2\pi x/a)$ where a is the lattice period. The same parameters (e.g., $a = 5.86$ Å) will be used as used previously[5] to illustrate the exact envelope-function method. The band structure of the well material ($V_0 = 0.746$ eV and $V_S = 2.7512$ eV, band gap 0.750 eV) is given in Fig. 1. The band structure for the barrier material ($V_0 = 0.0$ eV and $V_S = 5.0596$ eV, band gap 2.060 eV) is similar. The conduction-band offset is 230.1 meV. This relatively small band offset (compared to the band-gap difference of 1.310 eV) is chosen so that the energy-dependent effective-mass approximation to the band structure for both well and barrier crystals is reasonable for energies between the conduction-band edges. However, there is a significant difference between the zero wave-vector Bloch functions for the well and barrier crystals. This is illustrated in Fig. 2 where the zero wave-vector conduction-band Bloch functions for the well and barrier crystals are compared. To quantify the difference, consider the energy of the barrier-crystal conduction-band edge expressed as the expectation value $\langle U_c | H | U_c \rangle$ where H and U_c are, respectively, the Hamiltonian and the zero wave-vector conduction-band Bloch function for the barrier. When U_c for the barrier is replaced by the corresponding quantity for the well in this calculation, the expectation value falls by 102 meV. Considering that we need to be able to calculate energies to within a few meV, it is clear that we cannot, in general, ignore the difference between the Bloch functions of the well and

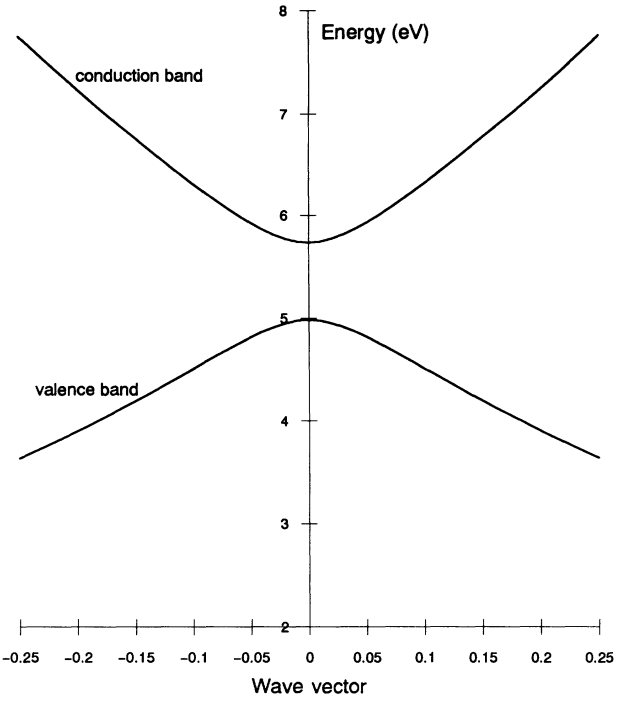

FIG. 1. Band structure of the crystal forming the well of the model one-dimensional superlattice. Only the second and third band are shown and these are labeled valence band and conduction band for convenient nomenclature. The wave vector is in units of $2\pi/a$, so that 0.5 corresponds to the zone edge. The plot here covers the inner half of the first Brillouin zone.

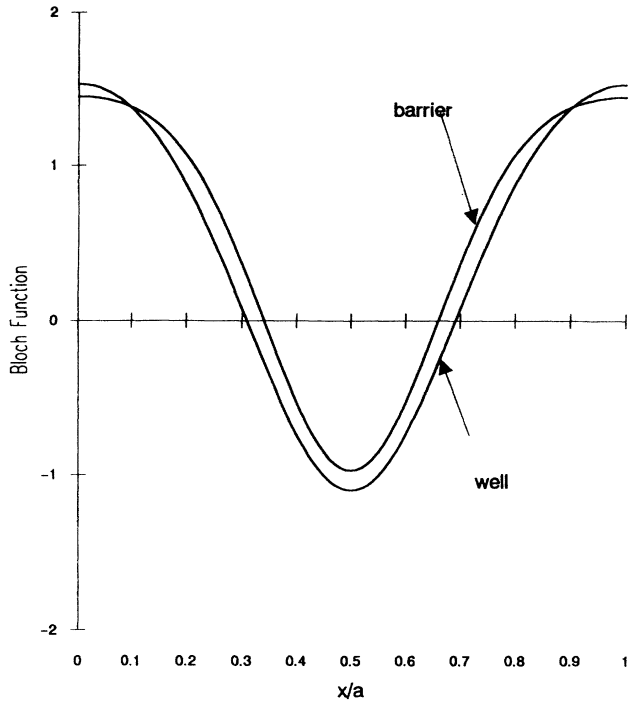

FIG. 2. Zero wave-vector conduction-band Bloch functions for the well and barrier crystals. They are normalized so that $\int_0^a U_c^* U_c dx/a = 1$.

barrier crystals for superlattices constructed from these crystals.

To construct the effective-mass approximation to the wave function of the ground state for the conduction band of the "Mathieu" superlattice described above, one can use the one-dimensional version of the algebraic results of the previous section with little modification. Because the microscopic potential of a "Mathieu" crystal is symmetric about the center of the unit cell, the zero wave-vector Bloch functions are either even or odd. Since the conduction-band state at zero wave vector is even, we can use (23a) for the envelope functions associated with even periodic basis functions and (23b) for those associated with odd periodic basis functions. The solution of the effective-mass Eq. (24) and use of the auxillary Eqs. (23a) and (23b) allow one to construct the wave function from (16). The exact wave functions have been computed by diagonalizing the plane-wave Hamiltonian (see, e.g., Eq. (4.8) in Ref. 5) using reciprocal lattice vectors of magnitude 5 or less in units of $2\pi/a$.

In the calculations described below, the well zero wave-vector Bloch functions have been chosen as the periodic basis functions U_n. In the well, $m_c(E,x)$ and $H_{cc}^{(2)}(E,x)$ correspond exactly to the well-bulk effective mass and the well-bulk conduction-band edge [the off-diagonal elements of $H_{nn'}(x)$ are all zero]. In the barrier $m_c(E,x)$ and $H_{cc}^{(2)}(E,x)$ will differ slightly from the bulk-barrier effective mass and the bulk-barrier conduction-band edge because the momentum matrix elements in $m_c(E,x)$ are those for the well not the barrier and the off-diagonal elements of $H_{nn'}(\mathbf{r})$ are nonzero. For instance, at the barrier band edge, $m_c(E,x)$ is 0.1122 in units of the free-electron mass and $H_{cc}^{(2)}(E,x)$ is 5.9559 eV. The corresponding values for the effective mass and the conduction-band edge in the barrier are 0.1285 and 5.9634 eV. Replacing $m_c(E,x)$ and $H_{cc}^{(2)}(E,x)$ in the barrier by the barrier effective mass and the barrier band-edge energy makes little difference in the wave function generated.

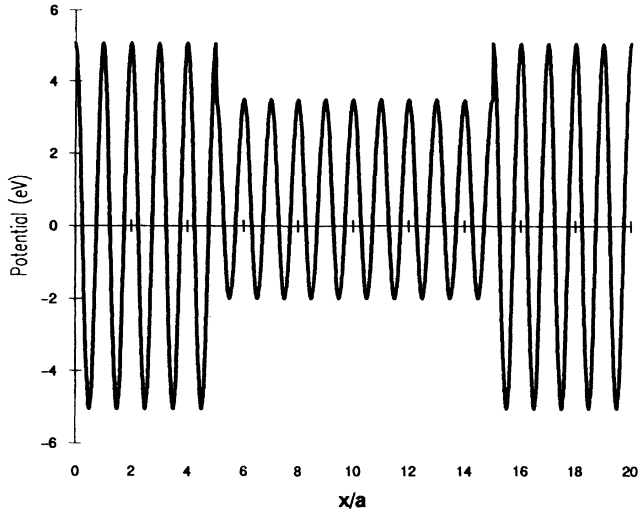

FIG. 3. Microscopic potential for the 10×10 superlattice. The origin is taken at the center of the barrier.

10×10 superlattice

The microscopic potential for this superlattice is plotted in Fig. 3 and the wave function for the state in the lowest conduction subband with zero superlattice wave vector in Fig. 4. The wave function in the effective-mass approximation computed as described above is barely distinguishable from the exact wave function shown in Fig.

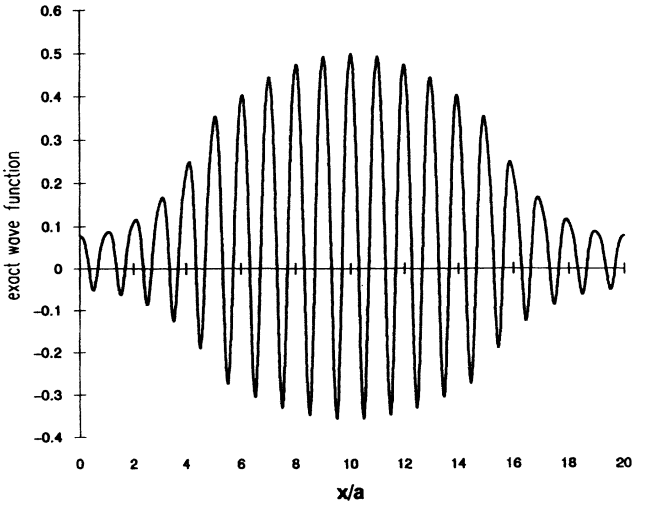

FIG. 4. Wave function for the lowest conduction-band state of the 10×10 superlattice. The wave function is normalized so that $\int_0^{20a} \psi^* \psi dx/a = 1$.

4. It is more informative to plot the deviations of the approximate wave function from the exact wave function and this is done in Fig. 5. The differences are remarkably small, a few percent at most. Indeed, in the well, where the electron spends most of its time (88%), the error is in the region of 2%. However, such an accuracy is required because the energy of the state, in the region of 5 eV, is large compared to the size quantization energies one is trying to calculate. A 2% error in the wave function produces a 0.04% error in the eigenvalue, i.e., 2 meV in 5 eV. (The actual error is 2.7 meV. See Ref. 5.) The differences in the well are somewhat larger than those in the barrier. The oscillatory behavior of the difference in the well is very similar to that of the conduction-band Bloch function (Fig. 2) and suggests that the approximate conduction-band envelope function is larger than the exact conduction-band envelope in the well region, but shows a much smaller deviation in the barrier. Examination of the approximate and exact conduction-band envelope functions shows that this is indeed the case. In Fig. 5 we also demonstrate the error incurred when the differences between the barrier and well Bloch functions is ignored. The dashed curve shows the difference in the effective-mass wave function and the exact wave function when the barrier Bloch functions are taken to be the same as the well Bloch functions, i.e., the corrections corresponding to Eq. (23a) are ignored. One sees that the errors in the wave function are now an order of magnitude higher leading to unacceptable errors (the energy is only 62.8 meV above the bulk-well conduction-band edge) even taking into account that the probability of finding the electron in the barrier is only 12%.

Figure 6 shows the exact envelope function and the effective-mass approximation thereto [calculated using the one-dimensional analogue of (23a)] corresponding to the lowest band. In the effective-mass approximation, this envelope function is zero in the well because there

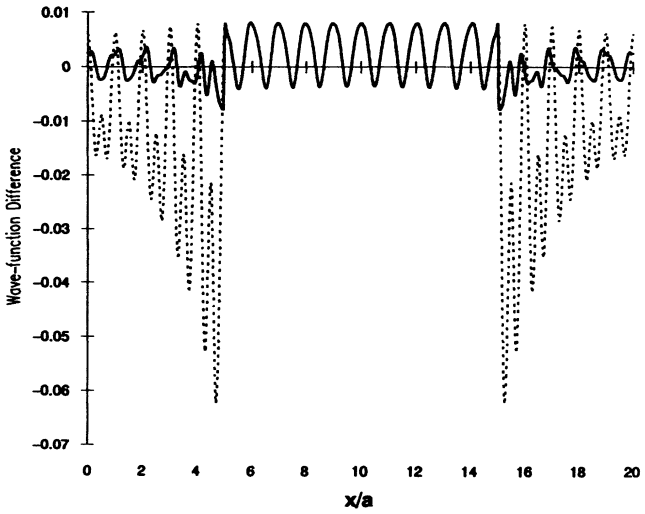

FIG. 5. The solid curve shows the difference between the approximate wave function and the exact wave function for the lowest conduction-band state of the 10×10 superlattice. The dashed curve shows how the approximation deteriorates if the well conduction-band Bloch function is substituted for that for the barrier.

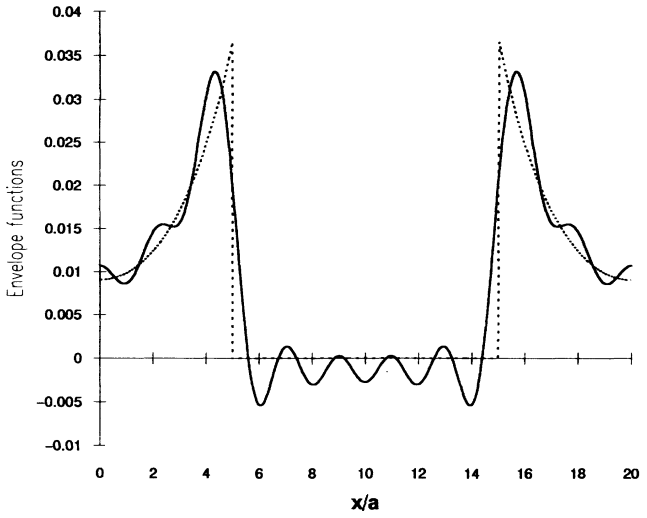

FIG. 6. Exact envelope function (solid curve) corresponding to the lowest band contribution to the envelope-function expansion (16) of the wave function depicted in Fig. 4. The dashed curve shows the effective-mass approximation for this envelope function.

are no off-diagonal elements of the Hamiltonian as the well zone-center Bloch functions form the basis. In the barrier, the off-diagonal matrix elements suddenly appear to take account of the fact that the zone-center Bloch functions for the barrier are different from those of the well. There is a corresponding jump in the envelope function at the interface. However, this discontinuous behavior is still a remarkably good approximation to the exact envelope function.

1×19 superlattice

In this case the electron, as we shall see, spends most of its time in the barrier crystal. The periodic basis functions are still chosen as the zero wave-vector Bloch functions for the wells so as to provide an extreme test of the approximation developed in this paper. One period of the microscopic potential is shown in Fig. 7 and the exact

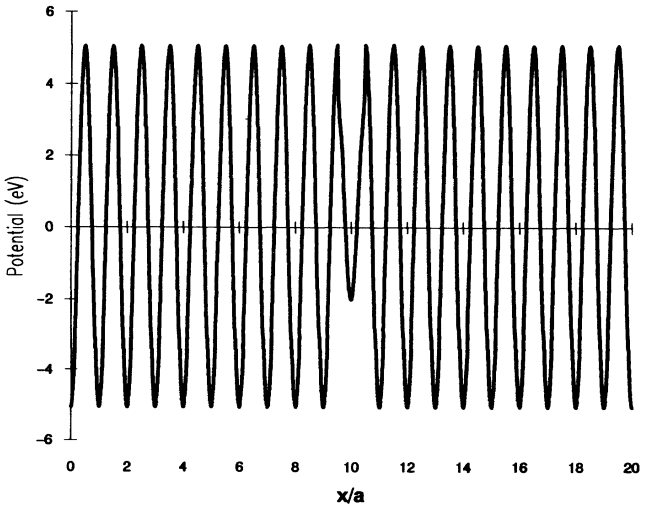

FIG. 7. Microscopic potential for the 1×19 superlattice. The origin is taken at the center of the barrier.

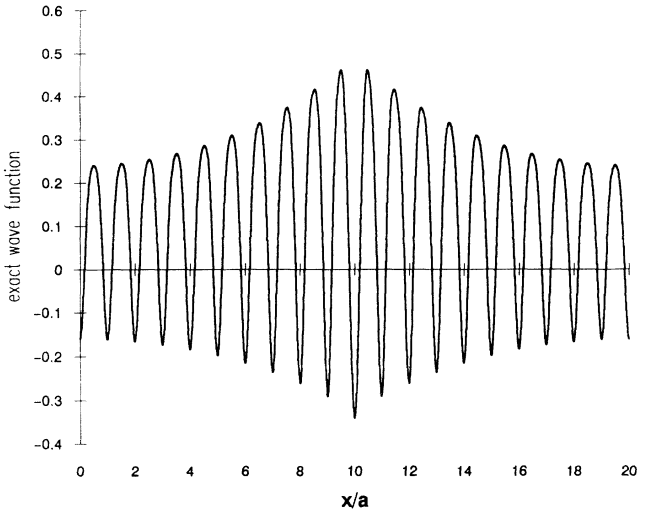

FIG. 8. Wave function for the lowest conduction-band state of the 1×19 superlattice. The wave function is normalized so that $\int_0^{20a}\psi^*\psi dx/a=1$.

wave function in Fig. 8. Again the errors in the effective-mass approximation to the wave function are too small to show the exact and approximate wave function clearly on the same graph so, in Fig. 9, the deviation of the approximate wave function from the exact wave function only are shown. Again the error in the wave function is remarkably small, and this is reflected in the approximate binding energy of 17.6 meV (relative to the barrier conduction-band edge) compared with the exact value of 15.1 meV. The comments made concerning the relative size of the errors in the well and barrier regions in Fig. 5 also apply in this case. Also shown is the error one would get in the wave function if the barrier Bloch

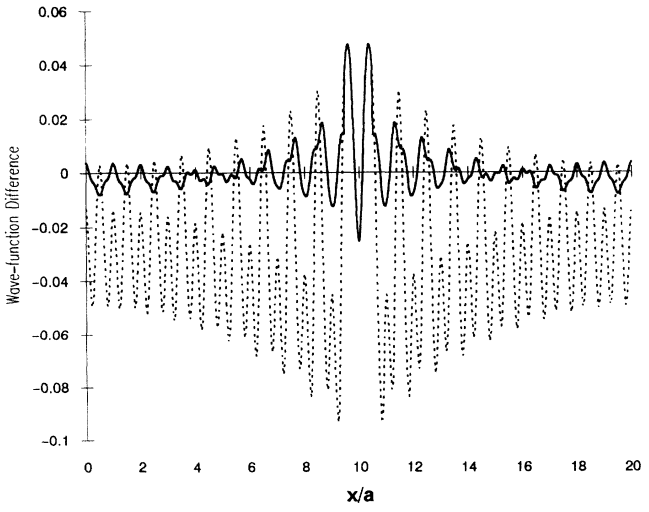

FIG. 9. The solid curve shows the difference between the approximate wave function and the exact wave function for the lowest conduction-band state of the 1×19 superlattice. The dashed curve shows how the approximation deteriorates if the well conduction-band Bloch function is substituted for that for the barrier.

functions are replaced by the well Bloch functions, i.e., the corrections corresponding to Eq. (23a) are ignored. Again the errors in the barrier region become unacceptably large.

Of course, if one wanted to get an approximation to the state shown in Fig. 8 using the hypothesis that the well and barrier zero wave-vector Bloch functions were interchangeable one would not use the well Bloch functions as a basis as was done here. One would clearly elect to take the barrier Bloch functions for the basis to minimize the error on the grounds that the electron spends most of its time in the barrier. The reason the above calculation was done the "hard" way was to magnify any shortcomings and hence emphasize how well the method copes with sudden changes in material composition; the fact that some of the envelope functions, albeit small ones, in the expansion (16) are discontinuous has not been a problem.

V. DISCUSSION AND SUMMARY

A feature of the derivation is that the order of the differential operators in the kinetic energy term arises naturally as part of the derivation and there has been no need to invoke heuristic *ad hoc* symmetrization procedures, which can lead to unphysical solutions for valence-band problems.[8] This ordering of the differential operators predicts that there will be a discontinuity in the derivative of the envelope function at an interface at which there is a discontinuity in the effective mass, the well-known effective-mass related kink in the envelope function. We can deduce this because we have established that (24) holds everywhere including boundaries. As demonstrated both algebraically[10] and numerically,[5] this kink approximates a real feature of the exact envelope function, namely a rapid change in the derivative in the neighborhood of the interface and that this feature is also manifest in the wave function.[5]

The main assumption in the derivation presented here is that the envelope functions are all slowly varying on the scale of the lattice period. However, the effective-mass equation obtained requires the principal envelope function to have a kink at an effective-mass discontinuity. Further, the small envelope functions are discontinuous at band-edge discontinuities. This would appear to create a problem because the approximate envelope functions do not have the fundamental property assumed. However, what is important to the derivation is that the dominant components in the plane-wave expansion of an envelope function have a small wave vector. The presence of a kink or discontinuity does not necessarily mean that this condition is violated. A discontinuity leads to plane-wave expansion coefficients varying as k^{-1} at large k while a kink leads to terms varying as k^{-2}.

A major step in the derivation is the approximation of the matrix elements of the microscopic potential with expressions that are valid for a small wave vector. Because of the abrupt nature of the boundaries the matrix elements vary, apart from phase factors, as the reciprocal of the wave vector. Hence, in taking the small wave-vector approximation, one is also retaining the dominant terms

in the Hamiltonian matrix regardless of whether the envelope functions are slowly varying or not. This is not to say that the effective-mass approximation will work no matter how rapid the envelope-function variation is, that is clearly not the case, but it does suggest that the approximation will not break down as quickly as one might expect as one considers situations in which the envelope functions vary more rapidly.

Another distinctive feature of this derivation of the effective-mass equation is that it provides a means of estimating the errors incurred by its use. The exact Schrödinger equation (3) has been approximated by omitting terms in the matrix element of the potential that have large wave-vector denominators. The error incurred could be estimated via perturbation theory if the ground-state wave function is known approximately. The latter can be calculated using the envelope-function expansion (16), the small envelope functions being generated by the auxillary equations (23a) and (23b).

In summary, an effective-mass equation, along with approximate envelope-function equations, has been derived for a microstructure with atomically abrupt interfaces without assuming that the difference between corresponding Bloch functions of the constituent materials can be neglected. The treatment also encompasses slowly graded crystals because the change in chemical composition from one atomic layer to the next must be abrupt, albeit small, in practice. The only assumptions made are that the envelope functions vary sufficiently slowly and, in the example treated explicitly, that one envelope function is dominant. Within these constraints there has been no restriction on the size of the constituent parts, e.g., the widths of the layers in a multilayer structure or the diameter of a quantum dot. The case of states in a conduction-band quantum well for a zinc-blende structure has been highlighted to emphasize the role of symmetry in the success of the particle in box method. The approximate effective-mass wave function has been computed for a one-dimensional model to demonstrate how the method can account for the difference in the Bloch functions of the component crystals even for quantum wells of monolayer dimensions.

ACKNOWLEDGMENT

The author would like to thank Dr. R. A. Abram for some helpful discussions. This paper arose out of an earlier manuscript largely based on Secs. I–III. The author would like to thank Witold Trzeciakowski for much perceptive and thought provoking comment on the earlier manuscript that resulted in the numerical work presented in Sec. IV and some of the comments made in Sec. V.

[1]G. Bastard, *Wave Mechanics Applied to Semiconductor Heterostructures* (Halstead, New York, 1988).

[2]G. Bastard, J. A. Brum, and R. Ferreira, *Solid State Physics: Advances in Research and Applications,* edited by D. Turnbull and H. Ehrenreich (Academic, New York, 1991), Vol. 44, p. 229.

[3]M. Altarelli, in *Heterojunctions and Semiconductor Superlattices,* edited by G. Allan, G. Bastard, N. Boccara, M. Lannoo, and M. Voos (Springer, Berlin, 1986), p. 12.

[4]G. A. Baraff and D. Gershoni, Phys. Rev. B **43**, 4011 (1991).

[5]M. G. Burt, J. Phys. Condens. Matter **4**, 6651 (1992).

[6]M. G. Burt, Semicond. Sci. Technol. **3**, 739 (1988).

[7]M. G. Burt, in *Bandstructure Engineering in Semiconductor Microstructures,* Vol. 189 of *NATO Advanced Study Institute, Series B: Physics,* edited by R. A. Abram and M. Jaros (Plenum, New York, 1989).

[8]B. A. Foreman, Phys. Rev. B **48**, 4964 (1993).

[9]See, e.g., Ref. 5 and 6. This method is just a variant of Löwdin's method as applied to renormalize $\mathbf{k}\cdot\mathbf{p}$ bandstructure matrices; see, e.g., E. O. Kane, in *Semiconductors and Semimetals,* edited by R. K. Willardson and A. C. Beer (Academic, New York, 1966), Vol. 1, p. 75.

[10]M. G. Burt, Semicond. Sci. Technol. **3**, 1224 (1988).